FEM Convergence for PDEs with Point Sources in 2-D and 3-D

Kourosh M. Kalayeh[1], Jonathan S. Graf[2], and Matthias K. Gobbert[2*]

[1]Department of Mechanical Engineering, University of Maryland, Baltimore County

[2]Department of Mathematics and Statistics, University of Maryland, Baltimore County

[*]Corresponding author: 1000 Hilltop Circle, Baltimore, MD 21250, gobbert@umbc.edu

Abstract: Numerical theory provides the basis for quantification of the accuracy and reliability of a FEM solution by error estimates on the FEM error vs. the mesh spacing of the FEM mesh. This paper presents techniques needed in COMSOL 5.1 to perform computational studies for elliptic test problems in two and three space dimensions that demonstrate this theory by computing the convergence order of the FEM error. In particular, we show how to perform these techniques for a problem involving a point source modeled by a Dirac delta distribution as forcing term. This demonstrates that PDE problems with a non-smooth source term necessarily have degraded convergence order compared to problems with smooth right-hand sides and thus can be most efficiently solved by low-order FEM such as linear Lagrange elements.

Keywords: Poisson equation, point source, Dirac delta distribution, convergence study, mesh refinement.

1 Introduction

The finite element method (FEM) is widely used as a numerical method for the solution of partial differential equation (PDE) problems, especially for elliptic PDEs such as the Poisson equation with Dirichlet boundary conditions

$$-\Delta u = f \quad \text{in } \Omega, \tag{1}$$

$$u = r \quad \text{on } \partial\Omega, \tag{2}$$

where $f(\mathbf{x})$ and $r(\mathbf{x})$ denote given functions on the domain Ω and on its boundary $\partial\Omega$, respectively. We assume the domain $\Omega \subset \mathbb{R}^d$ to be a bounded, open, simply connected, convex set in $d = 2$ or 3 space dimensions with a polygonal boundary $\partial\Omega$. Concretely, we consider $\Omega = (-1, 1)^d$, since this domain can be discretized by a FEM mesh consisting of triangles in 2-D or tetrahedra in 3-D without error.

The FEM solution u_h will typically incur an error against the PDE solution u of the problem (1)–(2). This can be quantified by bounding the norm of the error $u - u_h$ in terms of the mesh spacing h of the finite element mesh. Such estimates have the form, e.g., [1, Section II.7],

$$\|u - u_h\|_{L^2(\Omega)} \le C\, h^q, \quad \text{as } h \to 0, \tag{3}$$

where C is a problem-dependent constant independent of h and the constant q indicates the order of convergence of the FEM as the mesh spacing h decreases. We see from this form of the error estimate that we need $q > 0$ for convergence as $h \to 0$. More realistically, we wish to have for instance $q = 1$ for linear convergence, $q = 2$ for quadratic convergence, etc., where higher values yield faster convergence.

The norm $\|u - u_h\|_{L^2(\Omega)}$ in (3) is the L^2-norm associated with the space $L^2(\Omega)$ of square-integrable functions, that is, the space of all functions $v(\mathbf{x})$ whose square $v^2(\mathbf{x})$ can be integrated over all $\mathbf{x} \in \Omega$ without becoming infinite. The norm is defined concretely as the square root of that integral, namely $\|v\|_{L^2(\Omega)} := \left(\int v^2(\mathbf{x})\, d\mathbf{x}\right)^{1/2}$.

The result stated in (3) necessitates requirements on the finite elements used as well as on the PDE problem (1)–(2):

- Lagrange finite elements, such as those in COMSOL Multiphysics, approximate the PDE solution u at several points in each element K of a mesh $\mathcal{T}_h$, such that the restriction of u_h to each element K is a polynomial of degree up to p and $u_h(\mathbf{x})$ is continuous across all boundaries between neighboring elements throughout Ω. For the case of linear Lagrange elements with piecewise polynomial degree $p = 1$, the convergence order is $q = 2$ in (3), i.e., one higher than the polynomial degree; it also holds under additional assumptions on the PDE problem that for higher-order elements with degree p, the convergence order in (3) can reach $q = p + 1$.

Excerpt from the Proceedings of the 2015 COMSOL Conference in Boston

- One necessary assumption on the PDE is that the problem has a solution $u(\mathbf{x})$ that is sufficiently regular, as expressed by the number of derivatives it has. In the context of the FEM, it is appropriate to consider weak derivatives [1]. Based on these, we define the Sobolev function spaces $H^k(\Omega)$ of order k of all functions on Ω that have weak derivatives up to order k that are square-integrable in the sense of $L^2(\Omega)$ above. The convergence order q in (3) of the FEM with Lagrange elements with degree p is then limited by the regularity order k of the PDE solution as $q \leq k$.

These two facts above can be combined into the formula $q = \min\{k, p+1\}$ in (3). Thus, for linear Lagrange elements for instance, we need $u \in H^k(\Omega)$ with $k = 2$ to reach the optimal convergence order of $q = p + 1 = 2$.

The purpose of this paper is to show how one can demonstrate computationally the convergence order $q = p + 1 = 2$ for linear Lagrange FEM elements, if the PDE solution u is smooth enough (i.e., $k \geq 2$). Moreover, we demonstrate that the convergence order is indeed limited by $q \leq k$, if the solution is not smooth enough (i.e., $k < 2$). This latter situation arises concretely when considering a PDE with one (or more) point sources in the forcing term $f(\mathbf{x})$ on the right-hand side of (1). The reason is that the mathematical model for point sources is given by the Dirac delta distribution $\delta(\mathbf{x})$. This function is not square-integrable, and thus the PDE solution u is not in $H^2(\Omega)$.

In Section 2, we explain the numerical method applied to both smooth and a non-smooth problems in the following Sections 3 and 4, respectively. Specifically, Section 2 specifies how to initialize convergence studies with the coarsest meshes possible in two and three space dimensions and how to develop a computable estimate $q^{(\text{est})}$ of the convergence order q in (3) by regular mesh refinements. Section 3 shows the results for the convergence studies with smooth PDE solutions, which demonstrate that $q = 2$ in both two and three space dimensions of the PDE domain $\Omega \subset \mathbb{R}^d$. By contrast, Section 4 shows that for (1) with $f = \delta$ as forcing term, the convergence is limited in a dimension-dependent way, namely to $q = 1.0$ in two and $q = 0.5$ in three dimensions. In [2], we provide detailed instructions for obtaining the results of this report in COMSOL 5.1.

2 Numerical Method

One well-known, practical test for reliability of a FEM solution is to refine the FEM mesh, compute the solution again on the finer mesh, and compare the solutions on the two meshes qualitatively. The FEM theory provides a quantification of this approach by comparing FEM errors $u - u_h$ involving the PDE solution u compared to FEM solutions on meshes, whose mesh spacings h are related by regular mesh refinement. We use this theory here for linear Lagrange elements as provided in COMSOL Multiphysics. Since the domains $\Omega = (-1, 1)^d$ have polygonal boundaries, they can be discretized by triangular meshes in $d = 2$ and by tetrahedral meshes in $d = 3$ dimensions without error. The convergence studies performed rely on a sequence of meshes with mesh spacings h that are halved in each step. This is accomplished by uniformly refining an initial mesh repeatedly, starting from a minimal initial mesh to allow as many refinements as possible. For the initial mesh, we take advantage of the shape of Ω that admits a very coarse, uniform mesh that still includes the origin $\hat{\mathbf{x}} = 0$ as a mesh point, which is needed later for the non-smooth problems in Section 4. In $d = 2$ dimensions, the initial mesh consists of 4 triangles with 5 vertices given by the 4 corners of Ω plus the center point. In $d = 3$ dimensions, the initial mesh has 28 tetrahedra with 15 vertices. Figures 1 (a) and (b) show the initial meshes for the two- and three-dimensional domains, respectively. Figures 2 (a) and (b) show the exploded view of the initial mesh in three-dimensional domain. While Figure 2 (a) shows the exploded view of initial mesh for whole domain, Figure 2 (b) shows the exploded view with some elements removed so that we can view the inside elements of the domain and confirm that the origin is indeed a point in the discretization. Instructions for generating these mesh views are included in [2].

The initial meshes are refined uniformly $m = 1, 2, \ldots$ times. For each mesh, we track the number of mesh elements N_e, the degrees of freedom (DOF) N of the linear Lagrange elements for that mesh (i.e., the number of vertices), and the mesh spacing h for each refinement level m from the initial mesh for $m = 0$ to the finest mesh explored, as summarized in Tables 1 (a) and (b). The solution plots in the following sections use the mesh with refinement level $m = 3$.

All test problems are designed to have a known true PDE solution $u(\mathbf{x}) = u_{\text{true}}(\mathbf{x})$ to allow for a direct computation of the error $u - u_h$ against the FEM solution and its norm in (3). The convergence order q is then estimated from these computational results by the following steps: Starting from the initial mesh, we refine it uniformly repeatedly. If the mesh spacing h is defined as the maximum side length of all elements, i.e., $h := \max_e h_e$, this procedure halves the value of h in each refinement. In two dimensions, regular mesh refinement sub-divides every triangle into 4 triangles. In three dimensions, the same halving of h occurs, however the regular mesh refinement sub-divides each tetrahedral element into 8 smaller tetrahedra. The number of elements N_e as well as the observed mesh spacing h in Tables 1 (a) and (b) exhibit the expected behavior associated with regular mesh refinement. Let m denote the number of refinement levels from the initial mesh and define $E_m := \|u - u_h\|_{L^2(\Omega)}$ as the error norm on refinement level $m = 0, 1, 2, \ldots$. Then assuming that $E_m = C\,h^q$ according to (3), the error for the next coarser mesh with mesh spacing $2h$ is $E_{m-1} = C\,(2h)^q = 2^q\,C\,h^q$. Their ratio is then $R_m = E_{m-1}/E_m = 2^q$ and $Q_m = \log_2(R_m)$ provides us with a computable estimate $q^{(\text{est})} = \lim_{r\to\infty} Q_m$ for q in (3) as $h \to 0$.

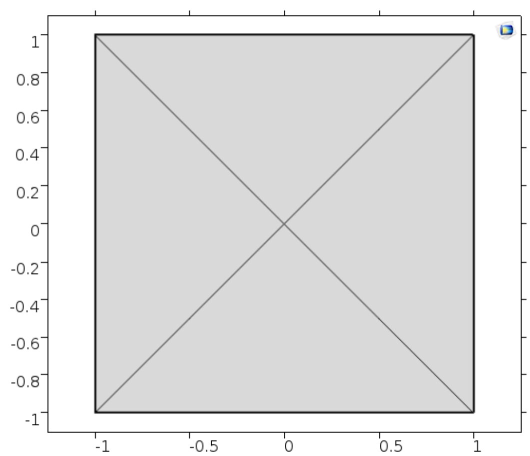

(a) $d = 2$

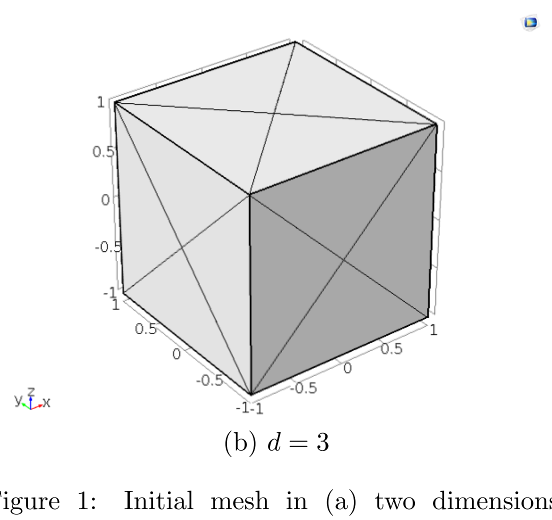

(b) $d = 3$

Figure 1: Initial mesh in (a) two dimensions, (b) three dimensions.

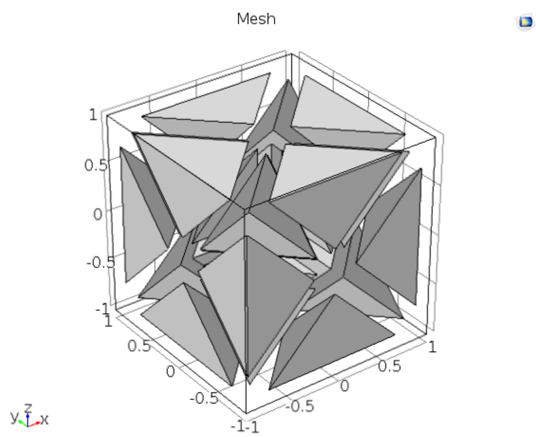

(a)

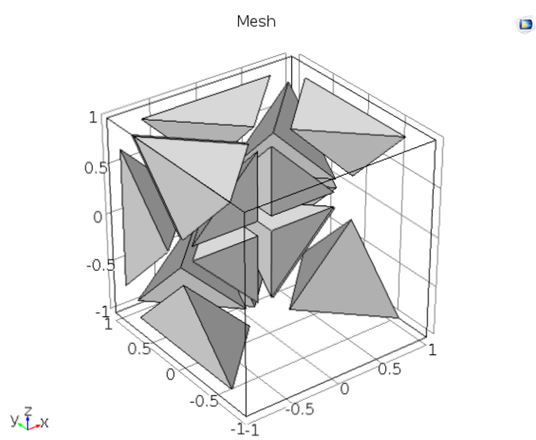

(b)

Figure 2: Exploded view of the initial mesh in three dimensions (a) for whole domain, (b) elements on one side removed to show interior elements of the domain.

Excerpt from the Proceedings of the 2015 COMSOL Conference in Boston

Table 1: Finite element data for all meshes in dimensions $d = 2$ and 3 for all refinement levels m.

m	N_e	$N = \text{DOF}$	h
0	4	5	2.0000
1	16	13	1.0000
2	64	41	0.5000
3	256	145	0.2500
4	1,024	545	0.1250
5	4,096	2,113	0.0625

(a) $d = 2$

m	N_e	$N = \text{DOF}$	$\max_e h_e$
0	28	15	2.0000
1	224	69	1.0000
2	1,792	409	0.5000
3	14,336	2,801	0.2500
4	114,688	20,705	0.1250
5	917,504	159,169	0.0625

(b) $d = 3$

3 Smooth Test Problems

For the smooth test problems, the right-hand side of Poisson equation $f(\mathbf{x})$ in (1) is chosen as

$$f(\mathbf{x}) = \begin{cases} \frac{\pi}{2}\left(\frac{1}{\rho}\sin\frac{\pi\rho}{2} + \frac{\pi}{2}\cos\frac{\pi\rho}{2}\right) & \text{for } d = 2, \\ \frac{\pi}{2}\left(\frac{2}{\rho}\sin\frac{\pi\rho}{2} + \frac{\pi}{2}\cos\frac{\pi\rho}{2}\right) & \text{for } d = 3, \end{cases}$$

where the norm $\rho = \sqrt{x^2 + y^2}$ in 2-D and $\rho = \sqrt{x^2 + y^2 + z^2}$ in 3-D. This function satisfies the standard assumption of $f \in L^2(\Omega)$ using in classical FEM theory [1, Chapter II]. This classical theory provides that u is two orders smoother, that is, $u \in H^2(\Omega)$, since $L^2(\Omega) \equiv H^0(\Omega)$ formally. The problems are chosen such that we know the PDE solutions

$$u_{\text{true}}(\mathbf{x}) = \begin{cases} \cos\frac{\pi\sqrt{x^2+y^2}}{2} & \text{for } d = 2, \\ \cos\frac{\pi\sqrt{x^2+y^2+z^2}}{2} & \text{for } d = 3, \end{cases} \qquad (4)$$

provided we choose the boundary condition function in (2) consistently as $r(\mathbf{x}) = u_{\text{true}}(\mathbf{x})$. Figures 3 (a) and (b) show two views of the FEM solution for mesh refinement $m = 3$.

The true PDE solutions $u_{\text{true}}(\mathbf{x})$ in (4) are infinitely often differentiable in the classical sense, and hence the regularity order $k = \infty$ does not limit the predicted convergence order $q = \min\{k, p+1\}$ for any degree p of the Lagrange elements. Specifically for linear Lagrange elements with degree $p = 1$, we expect to see $q = 2$ as convergence order for all spatial dimensions $d = 2, 3$. Table 2 lists for each refinement level m the error $E_m = \|u_h(\cdot,t) - u(\cdot,t)\|_{L^2(\Omega)}$ of (3) and in parentheses the estimate Q_m according to Section 2. We observe that Q_m approaches the value $q^{(\text{est})} = 2$, which is expected for a smooth source term in any spatial dimension $d = 2, 3$.

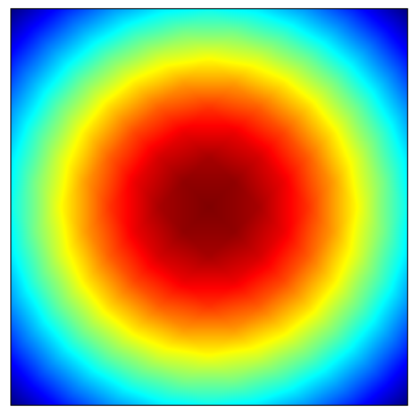

(a)

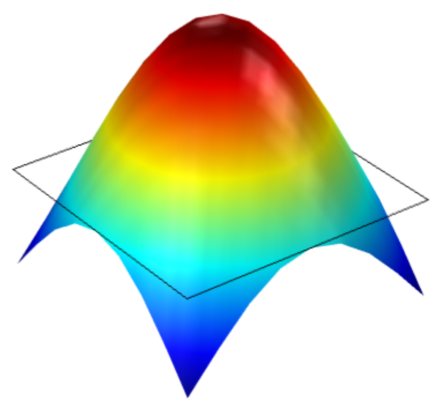

(b)

Figure 3: (a) Two-dimensional and (b) three-dimensional view of the FEM solution for the smooth test problem with $m = 3$.

Table 2: Convergence studies for the smooth test problem in two and three dimensions.

m	E_m (Q_m)
0	1.105
1	3.049e–01 (1.86)
2	8.387e–02 (1.86)
3	2.177e–02 (1.95)
4	5.511e–03 (1.98)
5	1.383e–03 (1.99)

(a) $d = 2$

m	E_m (Q_m)
0	1.132
1	3.481e–01 (1.70)
2	9.007e–02 (1.95)
3	2.273e–02 (1.99)
4	5.690e–03 (2.00)
5	1.422e–03 (2.00)

(b) $d = 3$

4 Non-Smooth Test Problems

For the non-smooth test problems, the forcing term $f(\mathbf{x})$ in (1) is chosen to model a point source. This is mathematically modeled by setting the forcing term as the Dirac delta distribution $f(\mathbf{x}) = \delta(\mathbf{x})$. The Dirac delta distribution models a point source at $\hat{\mathbf{x}} \in \Omega$ mathematically by requiring $\delta(\mathbf{x} - \hat{\mathbf{x}}) = 0$ for all $\mathbf{x} \neq \hat{\mathbf{x}}$, while simultaneously satisfying $\int \varphi(\mathbf{x})\, \delta(\mathbf{x} - \hat{\mathbf{x}})\, d\mathbf{x} = \varphi(\hat{\mathbf{x}})$ for any continuous function $\varphi(\mathbf{x})$. Based on the weak formulation of the problem, the finite element method is able to handle the source at $\hat{\mathbf{x}} = 0$ modeled by $f(\mathbf{x}) = \delta(\mathbf{x})$ in (1). That is, when the PDE is integrated in the derivation of the FEM with respect to a continuous test function $v(\mathbf{x})$, the right-hand side becomes $\int_\Omega v(\mathbf{x})\, \delta(\mathbf{x})\, d\mathbf{x} = v(0)$. If the point $\hat{\mathbf{x}} = 0$ is chosen as a mesh point of the FEM mesh, then the test function of the FEM with Lagrange elements evaluated at 0 in turn will equal 1 for the FEM basis function $v(\mathbf{x})$ centered at this mesh point and 0 for all others. This is the background behind the instructions in the COMSOL documentation to implement a point source modeled by the Dirac delta distribution by entering 1 as source function value at that mesh point. These instructions can be located by searching for "point source" in the COMSOL documentation.

Also for these problems exist closed-form PDE solutions $u_{\text{true}}(\mathbf{x})$, namely

$$u_{\text{true}}(\mathbf{x}) = \begin{cases} \frac{-\ln\sqrt{x^2+y^2}}{2\pi} & \text{for } d = 2, \\ \frac{1}{4\pi\sqrt{x^2+y^2+z^2}} & \text{for } d = 3, \end{cases} \tag{5}$$

provided we again choose the boundary condition function in (2) consistently as $r(\mathbf{x}) = u_{\text{true}}(\mathbf{x})$. Figures 4 (a) and (b) show two views of the FEM solution for mesh refinement $m = 3$. The FEM solution in the plots approaches the true solution, but the linear patches of the Lagrange elements with $p = 1$ are still clearly visible here. Notice that the true PDE solutions have a singularity at the origin 0, where they tend to infinity. Thus, the solutions are not differentiable everywhere in Ω and thus not in any space of continuous or continuously differentiable functions. However, recall the Sobolev Embedding Theorem [3]. Since $\int \varphi(\mathbf{x})\, \delta(\mathbf{x})\, d\mathbf{x} = \varphi(0)$ for any continuous function $\varphi(\mathbf{x})$, and the Sobolev space $H^{d/2+\varepsilon}$ is continuously embedded in the space of continuous function $C^0(\Omega)$ in $d = 1, 2, 3$ dimensions for any $\varepsilon > 0$, one can argue that δ is in the dual space of $\varphi \in H^{d/2+\varepsilon}(\Omega)$, that is, $\delta \in H^{-d/2-\varepsilon}(\Omega)$. Since the solution u of this second-order elliptic PDE is two orders smoother, we obtain the regularity $u \in H^{2-d/2-\varepsilon}(\Omega)$ or $k \approx 2 - d/2$ in (3), which suggests to expect a dimension-dependent convergence order $q = 2 - d/2$ for $d = 2, 3$ dimensions [4, 5].

Table 3 presents the error norm E_m as well as the observed Q_m in parentheses. For $d = 2$ dimensions in Table 3 (a), we see that Q_m approaches the value $q^{(\text{est})} = 1.0$, while for $d = 3$ dimensions in Table 3 (b), it approaches the value 0.5, which indeed agrees with the expected order $q = 2 - d/2$.

5 Conclusions

In this paper, the test problems are Poisson equations with smooth or non-smooth solutions. With true PDE solution available, we can calculate errors with the FEM solution against the PDE solution. For the smooth test problems, the convergence order is 2 in all dimensions $d = 2, 3$. In the non-smooth test problems, the results agree with the theoretical expectation that convergence order is reduced in a dimension-dependent way to $q = 1.0$ in two and $q = 0.5$ in three dimensions. Therefore, linear Lagrange elements, which require less computational effor than higher-order elements, are op-

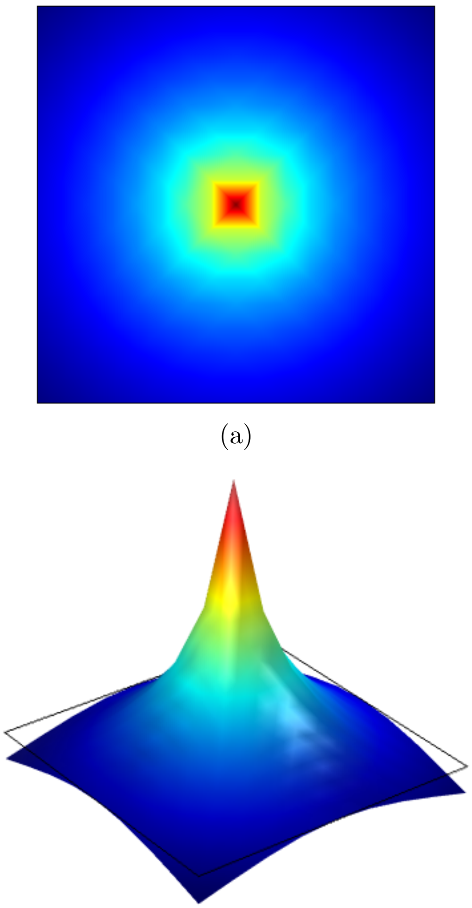

(a)

(b)

Figure 4: (a) Two-dimensional and (b) three-dimensional view of the FEM solution for the non-smooth test problem with $m = 3$.

timal for problems involving point sources modeled by Dirac delta distributions.

Acknowledgments

The hardware used in the computational studies is part of the UMBC High Performance Computing Facility (HPCF). The facility is supported by the U.S. National Science Foundation through the MRI program (grant nos. CNS–0821258 and CNS–1228778) and the SCREMS program (grant no. DMS–0821311), with additional substantial support from the University of Maryland, Baltimore County (UMBC). See hpcf.umbc.edu for more information on HPCF and the projects using its resources. Co-author Graf acknowledges financial support as HPCF RA.

Table 3: Convergence studies for the non-smooth test problem in two and three dimensions.

m	E_m (Q_m)
0	9.332e–02
1	4.589e–02 (1.02)
2	2.468e–02 (0.89)
3	1.256e–02 (0.97)
4	6.311e–03 (0.99)
5	3.160e–03 (1.00)

(a) $d = 2$

m	E_m (Q_m)
0	1.026e–01
1	6.990e–02 (0.55)
2	4.842e–02 (0.53)
3	3.410e–02 (0.51)
4	2.410e–02 (0.50)
5	1.704e–02 (0.50)

(b) $d = 3$

References

[1] Dietrich Braess. *Finite Elements*. Cambridge University Press, third edition, 2007.

[2] Kourosh M. Kalayeh, Jonathan S. Graf, and Matthias K. Gobbert. FEM convergence studies for 2-D and 3-D elliptic PDEs with smooth and non-smooth source terms in COMSOL 5.1. Technical Report HPCF–2015–19, UMBC High Performance Computing Facility, University of Maryland, Baltimore County, 2015.

[3] Michael Renardy and Robert C. Rogers. *An Introduction to Partial Differential Equations*, vol. 13 of *Texts in Applied Mathematics*. Springer-Verlag, second edition, 2004.

[4] Ridgway Scott. Finite element convergence for singular data. *Numer. Math.*, vol. 21, pp. 317–327, 1973.

[5] Thomas I. Seidman, Matthias K. Gobbert, David W. Trott, and Martin Kružík. Finite element approximation for time-dependent diffusion with measure-valued source. *Numer. Math.*, vol. 122, no. 4, pp. 709–723, 2012.